Environmental Studies by Multispectral Scanner of a Large-scale Civil Engineering Construction Area

Rikimaru, Atsushi / 大嶋, 太市 / 力丸, 厚 / 竹内, 章司 / Oshima, Taichi / Takeuchi, Shoji

(出版者 / Publisher)
法政大学工学部
(雑誌名 / Journal or Publication Title)
法政大学工学部研究集報 / 法政大学工学部研究集報
(巻 / Volume)
18
(開始ページ / Start Page)
79
(終了ページ / End Page)
90
(発行年 / Year)
1982-03
(URL)
https://doi.org/10.15002/00004103

Environmental Studies by Multispectral Scanner of a Large-scale Civil Engineering Construction Area

Dr. Shoji TAKEUCHI*, Atsushi RIKIMARU**
and Prof. Dr. Taichi OSHIMA***

Abstract

This paper describes a technical approach using airborne multispectral scanner (MSS) data for the evaluation of the vitality of forest trees for the purpose of environmental monitoring of a forested area under long tunnel construction. The study has been conducted over the past four years (1977–1981) using airborne 11 channel MSS data acquired once in early October each of these years.

The emphasis of the study is on the development of pre-processing tools of MSS data and a basic experiment on the relationship between the spectral characteristics and the vitality of some tree samples, both of which are basic tasks to achieve a reliable evaluation of tree vitality change with the MSS.

As a result of evaluations using several algorithms, no essential yearly change of tree vitality was yet recognized in the test site, although seasonal variations in deciduous trees and artificial changes caused by forest management were detected by the MSS data.

1. Introduction

Thi study was initiated due to the environmental impact caused by a large-scale civil engineering construction project. In the test site, tunnel construction has been in progress over a six kilometer length and it had caused underground water flooding, resulting in long-term environmental change of vegetal and soil moisture conditions at this site which could be monitored by both ground survey techniques and remote sensing.

Since forest trees occupy more than 70 percent of hte total vegetation area of the test site, the main target of this study has been focused on the vitality of forest trees. The monitoring of tree vitality by remote sensing was done generally using aerial color photographs until now. However, in this study, an airborne multispectral scanner (MSS) has been used because of its merit in quantitative data acquisition. Since the use of MSS data for such monitoring is still in an experimental stage, the main focus of this study has been the development of data analysis tools and the establishment of evaluation algorithems for MSS data in order to achieve reliable monitoring by MSS.

2. Approach

The experimental approach is illustrated in Fig. 1. To improve the reliability of monitoring

* Remote Sensing Technology Center of Japan: UNI Roppongi Bld., 7-15-17, Roppongi, Minato-ku, Tokyo, Japan 〒106

** Pacific Aero Survey Co. Ltd.: 2-13-5, Higashiyama, Meguro-ku, Tokyo, Japan 〒153

*** Dept. of Civil Eng., College of Eng., Hosei University: 3-7-2- Kajino-cho, Koganei-shi, Tokyo, Japan 〒184

with a MSS, the following experimental tasks were carried out:

a) maintaining year-to-year compatibility of MSS data acquisition.

b) establishing in-situ ground measurement of spectral reflectance and radiometric temperature in order to obtain the calibration source of MSS data.

c) developing radiometric and geometric data correction techniques in order to improve the accuracy of year-to-year comparison of of MSS data.

d) establishing the relationship between tree vitality change and spectral change of trees using some tree samples in order to obtain evidence for justification of monitoring with a MSS.

3. MSS Data Acquisition and In-situ Ground Measurement

Eleven-channel airborne MSS data was acquired once a year from 1977 to 1981 at the test site. Fig. 2 shows the scheme of data acquisition. The flight course was along the tunnel line and the altitude was 1000 meters above the average ground surface.

In order to maintain year-to-year compatibility of acquired data, attempts were made to acquire MSS data under the same conditions such as season, time of day and altitude and flight course, although the observation data had to be shifted slightly every year due to weather conditions. The observation dates were Oct. 2 in 1977, Sep. 25 in 1978, Oct. 10 in 1979 and Oct. 9 in 1980 and the observation time was from 10 to 12 a.m..

Table 1 shows the wavelength characteristics of the MSS channels. A Bendix Modular Multi-

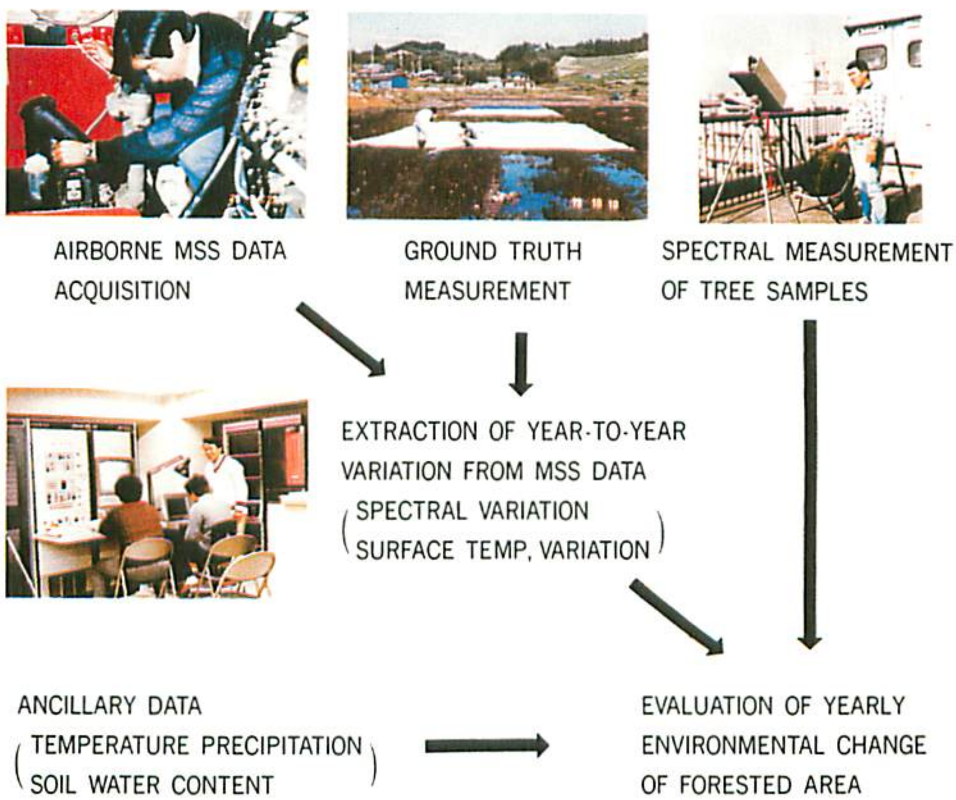

Fig. 1 Illustration of experimental approach.

Table 1 Channel No. and wavelength (μm) of MSS

No.	Wavelength	No.	Wavelength	No.	Wavelength
1	0.38-0.44	5	0.58-0.62	9	0.77-0.86
2	0.44-0.49	6	0.62-0.66	10	0.97-1.06
3	0.49-0.54	7	0.66-0.70	11	8.0 -1.30
4	0.54-0.58	8	0.70-0.74		

band Scanner (M^2S) was used from 1977 to 1979 and a Daedalus DS-1250 was used in 1980. The latter has slightly different wavelength characteristics from those shown in Table-1.

At the time of MSS data acquisition, ground measurements on spectral reflectance and radiometric temperature were carried out using several artificial and natural targets. The artificial targets were three or four sheets of cloth 10m×10m in size and having different levels of grey. The natural targets were ponds or rivers, concrete, bare soil, paddy fields, and so on. Measured ground data were used for the calibration of the MSS data described in section 5.

4. Basic Experiment on Spectral Characteristics of Tree Samples

Fundamental to the evaluation of tree vitality by spectral characteristics is chlorophyll, which is an important carrier of solar energy in the photosynthesis process and consequently, its activity is closely related to the biological activity of vegetation. Also active chlorophyll pigment has an established characteristic spectral reflectance pattern. The purpose of this experiment was to verify the change of spectral characteristics due to the change of the biological condition of trees and to obtain spectral evidence for the evaluation of tree vitality by remote sensing.

The experimental method was to measure the spectral reflectance values of sampled trees and to measure these from fresh dead. The spectral reflectance was measured using a spectral

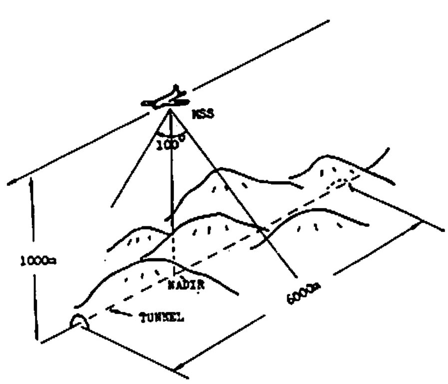

Fig. 2 Schematic description of MSS data acquisition.

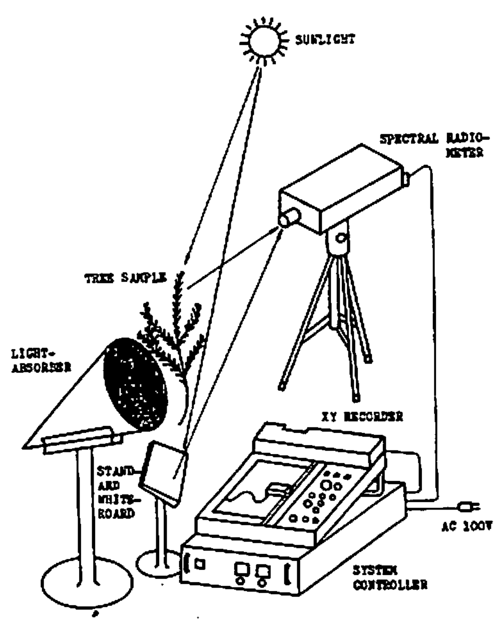

Fig. 3 Equipment and its configuration for spectral measurement of tree samples.

radiometer and a standard white board. The spectroscopic element of the radiometer is a diffraction grating and the range of spectral windows is from 400 nm to 900 nm with the band width smaller than 10 nm. Fig. 3 shows the configuration of the equipment and tree samples. The samples were of red pine, a dominant tree species in the test site, which had been taken

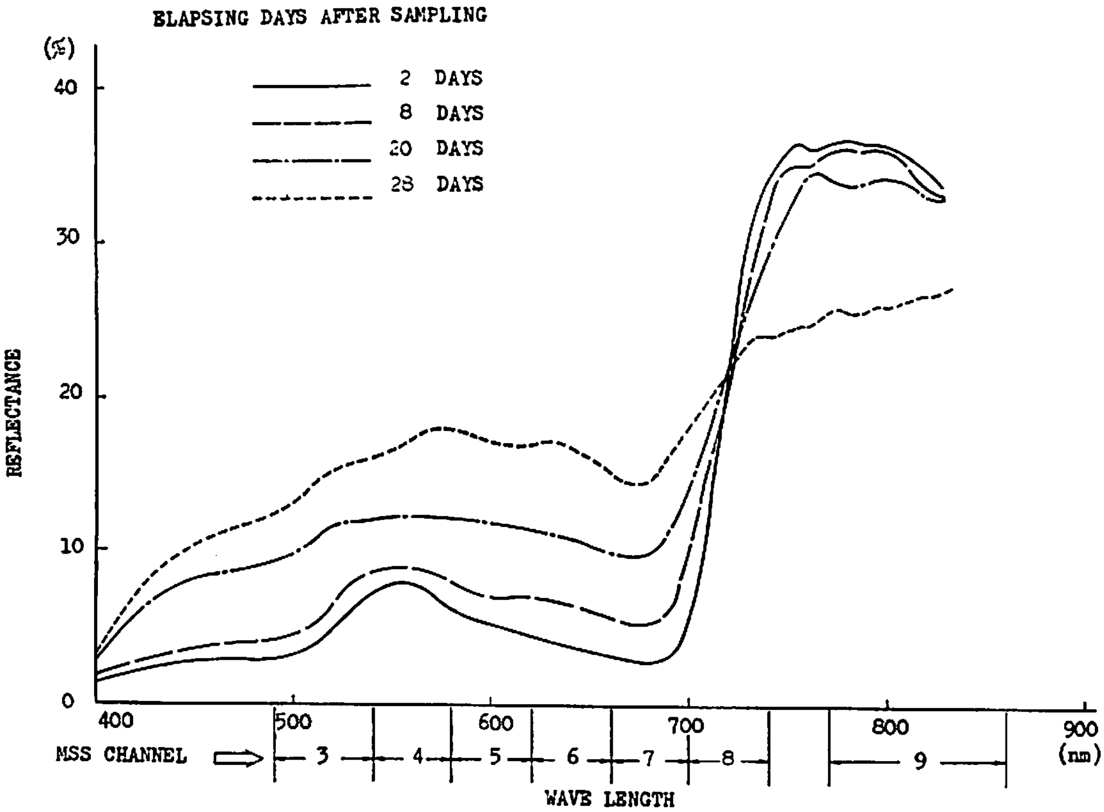

Fig. 4 Temporal change of spectral characteristics of unwatered red pine.

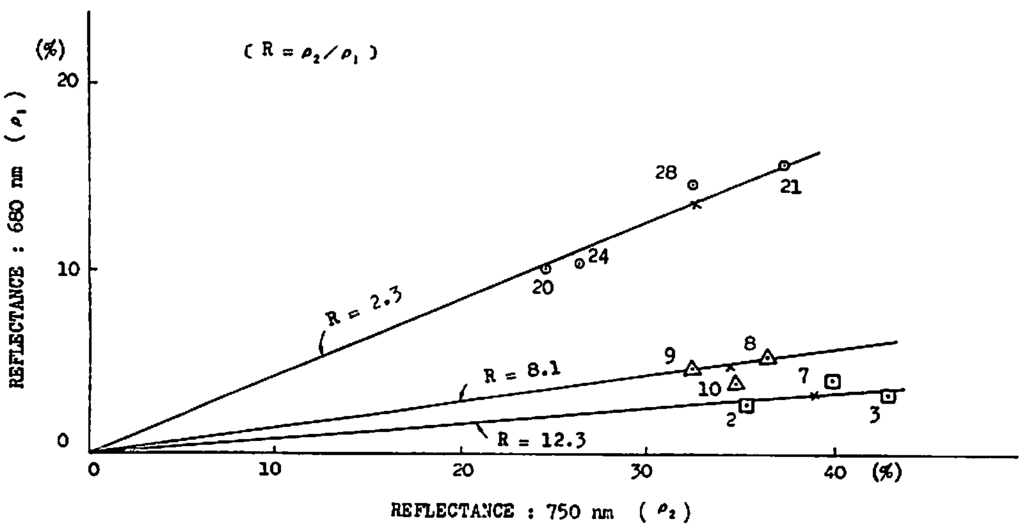

Fig. 5 Temporal change of bi-band ratio of unwatered red pine. The figure of each point represents the elapsed days after sampling. × shows the average value among each group (⊡, △ and ⊙).

from the test site to the laboratory.

Fig. 4 shows the temporal change of the spectral reflectance pattern of tree samples about a month after sampling. Since the sample was not supplied with water, it seasoned gradually and finally died. Fig. 4 shows that a healthy (high vitality) condition is characterized by the following spectral features;

(1) Convex pattern at 550 nm

(2) Low reflectance value at 680 nm.

(3) High reflectance value from 750 nm to 800 nm.

Fig. 5 shows the characteristic of the bi-band ratio defined as follows;

$R=\rho_2/\rho_1$

(ρ_1: Reflectance at 680 nm)

(ρ_2: Reflectance at 750 nm)

From Fig. 5, the decrease of tree vitality is characterized by the decrase of R, that is, when fresh R is around 12, then R falls below 8 with seasoning and finally R reaches about 2 when dead.

From the point of view of MSS data applicaiton, the results of this experiment suggest that effective channels for the detection of tree vitality change are channel 7 and channel 9 in Table-1. Though channel 9 does not cover 750 nm, it covers around 800 nm where spectral behavior is almost the same as those at 750 nm, and so, it is more suitable than either channel 8 or channel 10.

5. MSS Data Correction and Calibration

A complete flow diagram of MSS data analysis is shown in Fig. 6. The analysis process is mainly divided into two parts, the data correction and calibration process, and the process for the evaluation of tree vitality change. Data correction and calibration are the basic and important pre-processes in order to achieve the reliable evaluation of MSS data.

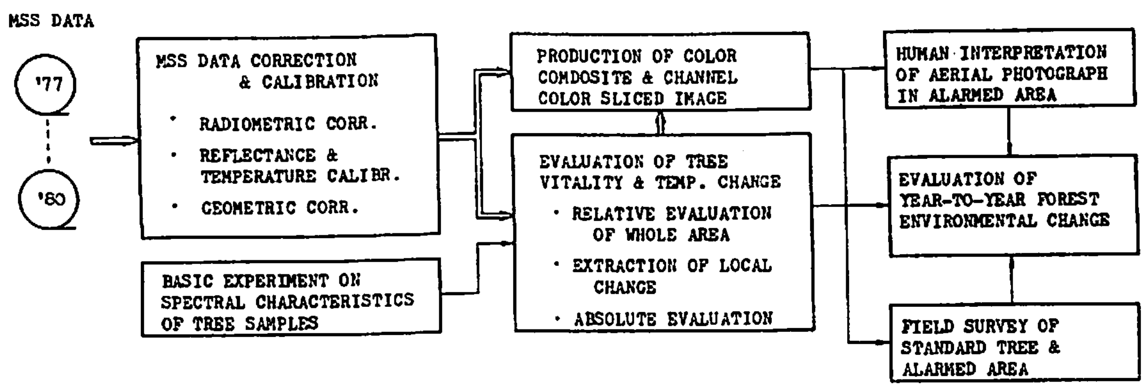

Fig. 6 Flow diagram of MSS data analysis for the evaluation of tree vitality change.

5.1 Radiometric Correction

Radiometric data correction is necessary to eliminate image distortion cased by temporal variation of solar radiaiton, spatial variation of path radiance effect, and lookangle effects of a scanner. The schematic descriptions for these distortion factors and their correction are shown in

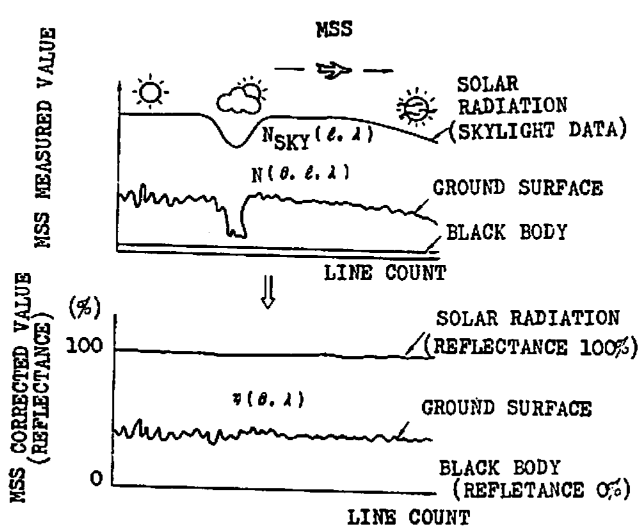

Fig. 7 Schematic description of data correction for the temporal variation of solar radiation.

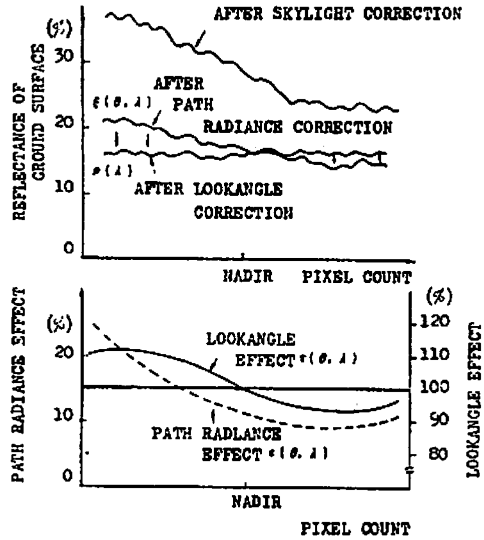

Fig. 8 Schematic description of data correction for the effects of path radiance and the lookangle of a scanner.

Fig. 7 and Fig. 8. This correction offers homogeneous data sources for reflectance calibration of each channel data (see 5.2) and for the extraction of year-to-year change from multi-year images (see 6.1).

The following simple linear model was introduced in order to carry out the correction;

$$N(\theta, \ell, \lambda)=\frac{1}{\pi}H(\ell, \lambda)\times\eta(\theta, \lambda) \quad \cdots\cdots(5.1)$$

$$\eta(\theta, \lambda)=\xi(\theta, \lambda)+\varepsilon(\theta, \lambda) \quad \cdots\cdots(5.2)$$

$$\xi(\theta, \lambda)=\tau(\theta, \lambda)\times\rho(\lambda) \quad \cdots\cdots(5.3)$$

where

$N(\theta, \ell, \lambda)$: Measured value of hte reflection of a ground object.
$\rho(\lambda)$: Inherent reflectance of the ground object.
$H(\ell, \lambda)$: Solar irradiance.
$\tau(\theta, \lambda)$: Lookangle effect of a scanner.
$\varepsilon(\theta, \lambda)$: Path radiance effect.
θ: Lookangle (Pixel count).
ℓ: Line count.
λ: Wavelength.

The distortion factors $H(\ell, \lambda)$, $\varepsilon(\theta, \lambda)$ and $\tau(\theta, \lambda)$ are approximated as follows;

$$\frac{1}{\pi}H(\ell, \lambda)\simeq N_{SKY}(\ell, \lambda)/K(\lambda) \qquad \varepsilon(\theta, \lambda)\simeq \min_{\theta}(\eta(\theta, \lambda))$$

$$\tau(\theta, \lambda)\simeq \operatorname{avr}_{\theta}(\xi(\theta, \lambda))/\operatorname{avr}_{\theta_0}(\xi(\theta, \lambda))$$

where

$N_{SKY}(\ell, \lambda)$: Measured value of solar radiation by MSS (Skylight data).
$K(\lambda)$: Çalibration coefficient of $N_{SKY}(\ell, \lambda)$.
$\min_{\theta}(\ )$: Minimum value along line count of lookangle

$\overset{avr}{\theta}(\ )$: Average value along line count of lookangle

θ_0: Lookangle at nadir of a scanner.

The correction was carried out sequentially from Eq. (5.1) to Eq. (5.3) and finally the reflectance $\rho(\lambda)$ was derived.

5.2 Reflectance and Temperature Caribration

Because of simplification and nonlinearity, $\rho(\lambda)$ derived by the above correction was not always equal to the real reflectance value of a ground object. The calibration for the derivation of real $\rho(\lambda)$ was carried out using several measured values of targets directly on the ground. The second-order regression curve with zero reflectance fixed was used as the calibration curve.

The MSS data of channel 11 represent the radiometric response of the surface of a ground object. However, because of atmospheric absorption, the carribration is also necessary for channel 11 data. Simple linear calibration using ground thermal targets was carried out to derive the radiometric response patern with a MSS.

5.3 Geometric Correction

Geometric data correciton was the basic process for spatial superposition of multi-year images for the mapping of images onto a topographical map. The schematic description of the correction is shown in Fig. 9. The following factors are introduced for the identification of pixel and line count (p_i, l_i) of a point $p_i(X_i, Y_i, Z_i)$;

Trajectory of nadir of a scanner: $Y_0=F_n(X_0)$

Scan direction angle: $\varphi_i=F_s(X_0)\simeq F_s(X_i)$,

Altitude: $h_i=F_a(X_0)$

Line count identification function: $\ell_i=F\ell(X_0)$

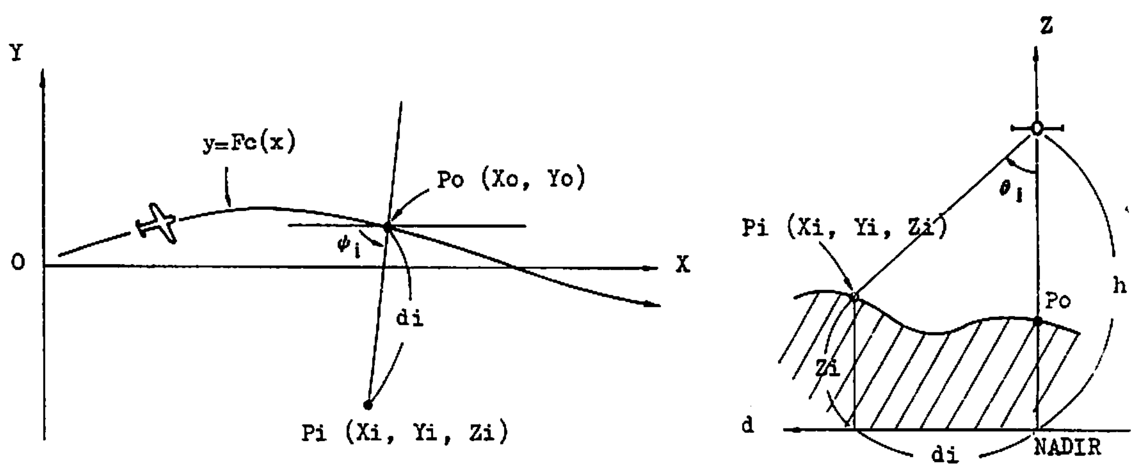

Fig. 9 Schematic description of geometric data correction.

These identification functions F_n, F_s, F_a and $F\ell$ are approximated by third-order regression curves, which are derived from thirty ground control points (GCP). The pixel count p_i is derived as follows;

$$p_i=K\theta_i+p_n,\quad \theta_i=\tan^{-1}(d_i/(h_i-Z_i)),\quad d_i=\sqrt{(X_i-X_0)^2+(Y_i-Y_0)^2}$$

Where K: Constant. p_n: pixel count at nadir of a scanner.

The identification error was about five pixels/line on the average. In order to obtain higher accuracy of identification, it was necessary to readjust the pixel and line count by affine transformation in a local seciton.

6. Evaluation of Year-to-Year Change of Tree Vitality

The evaluation process, which was carried out by using both the corrected or calibrated MSS data and the results of the basic experiment, is described in section 4. Since the experiment in section 4 has been done in a very simplified situation, it is necessary to examine various algorithms for applying the results of the experiment to actual complex forested areas, where various forest types are mixed. The authors have tried both "relative" and "absolute" evaluation algorithms. The former uses the relative spectral change as the index for tree vitality change; on the other hand, the latter uses the absolute value indicating the degree of tree vitality, that is, the value of the bi-band ratio of channel 7 to channel 9 of MSS data.

6.1 Relative Evaluation

Fig. 10 shows the schemaitc description for evaluation of the general change of tree vitality within a whole area. The rigid curves in the figure represent year-to-year regression curves with zero reflectance fixed, which were obtained from the data set of forest trees covering a whole area. The dotted lines represent the regression lines indicating the reflectance constant between two years, which were obtained from the data set of non-vegetal ground objects. The judgement about increase or decrease of tree vitality is done using the inverse deviation of regression curves from the reflectance constant both in channel 7 and 9.

Fig. 11 shows the actual result of application of the method described in Fig. 10 to the data set of forest trees in 1977 and 1978. The data set of the test site is divided into two sections (area A and B). In this case, the result shows the increase of tree vitality from 1977 to 1978 clearly in both A and B.

Fig. 12 shows another algorithms for relaitve evaluation, that is, for the extraction of local change from multi-year images. This algorithm utilizes a two step linear transformation technique of a single channel image to the other, which includes equalization of mean and variance and selective regression analysis using the residual image of the previous transformation. The combination of the results of extraction using both channels 7 and 9 are utilized for the evaluation of local changes of tree vitality.

Fig. 13 shows the results of the extraction of local changes from 1977 to 1978 and from 1978 to 1979. The figure also shows the local changes in channel 11, that is, the radiometric response pattern of tree surfaces. Note that a recovery process is indicated in some spots in the test site of the figure since one spot, which shows the decrease in vitality from 1977 to 1978, shows an increase in vitality from 1978 to 1979. In addition, the change in temperature patterns from 1977 to 1979 corresponds to the change of tree vitality in the following manner;

[Temperature up—Vitality decrease] [Temperature down—Vitality increase]

This correspondence suggests the feasibility for a more complicated evaluation process using the combination of visible, near-infrared and thermal channels.

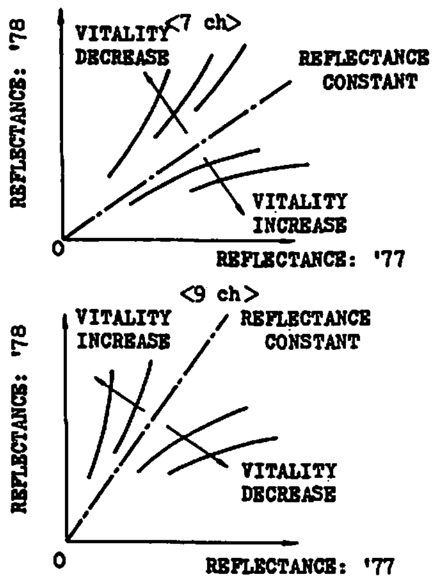

Fig. 10　Evaluation of general change of tree vitality.

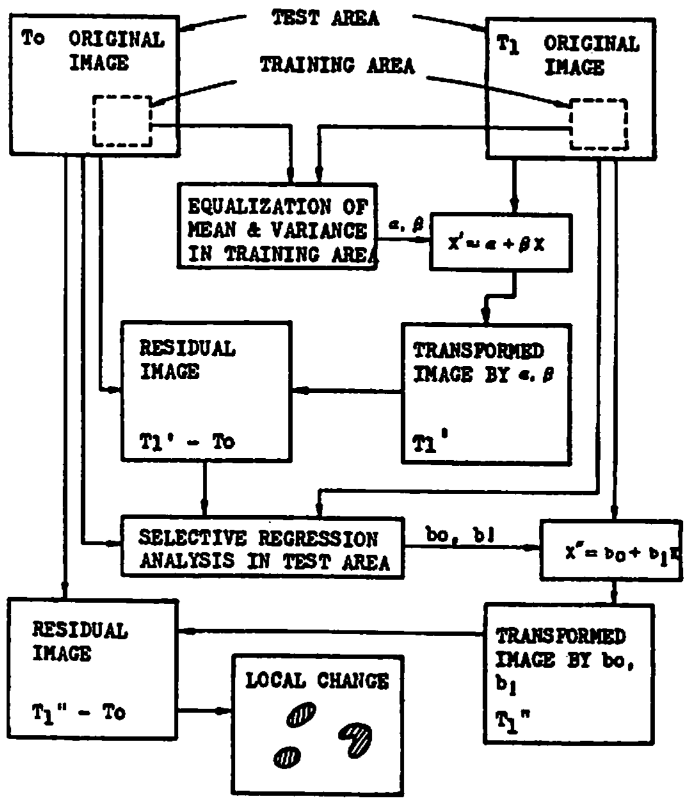

Fig. 12　Flow digaram for the extraction of local changes from multi-year images.

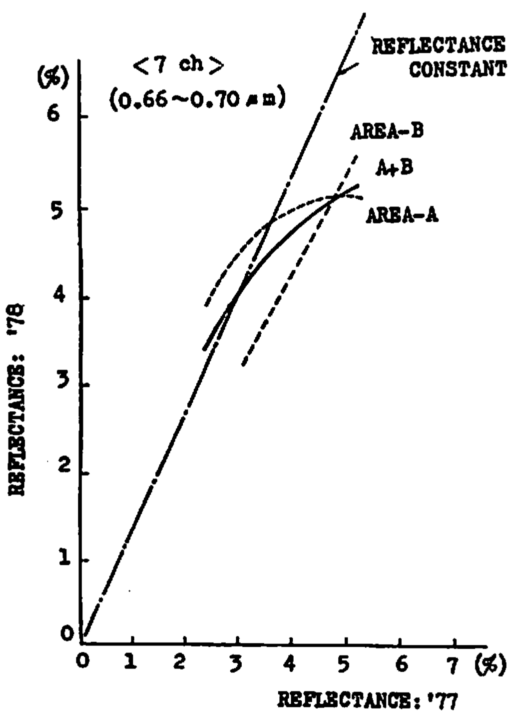

Fig. 11(a)　Regression curves of tree data set between 1977 and 1978 (channel 7)

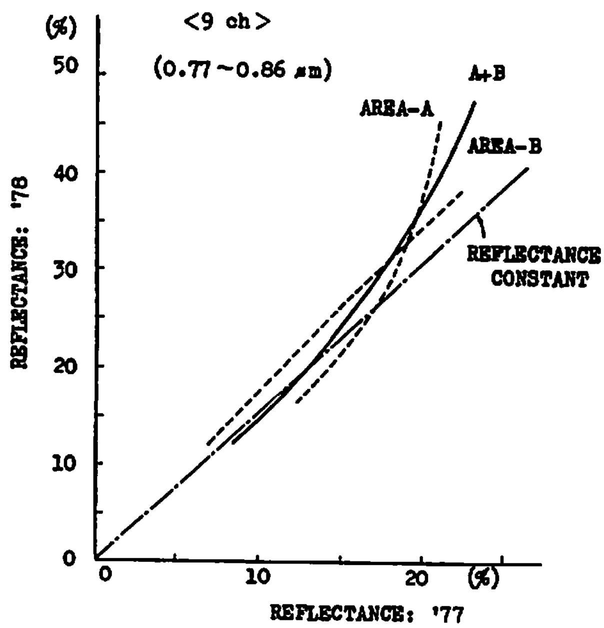

Fig. 11(b)　Regression curves same as (a) (channel 9)

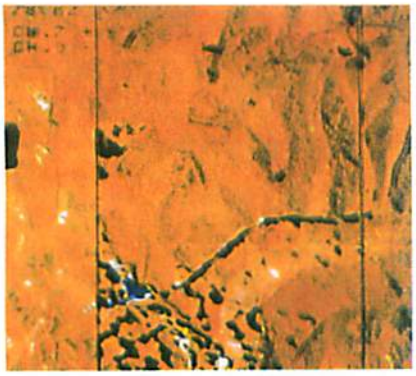

Decrease 7 CH^{+} 9 CH^{-} ('77-'78)

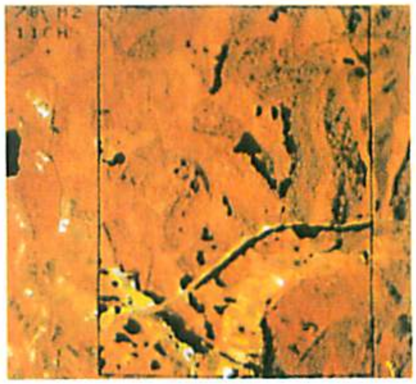

Increase 11 CH^{+} ('77-'78)

Increase 7 CH^{-} 9 CH^{+} ('78-79)
TREE VITALITY

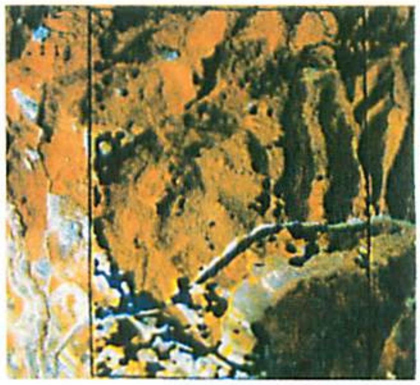

Decrease 11 CH^{-} ('78-79)
SURFACE TEMPERATURE

Fig. 13 Examples of the extraction of local changes in tree vitality and tree surface temperature from multi-year MSS images. The extracted spots are shown as blackened areas in every image.

6.2 Absolute Evaluation

The evaluaiton of the degree of tree vitality has been tried using the ratio of the calibrated reflectance data of channels 7 and 9. In Fig. 5 of section 4, the value of the ratio of (Channel 9/Channel 7) is about 8 to 12 for fresh free samples and about 2.3 to 8 for low vitality tree samples. The mapping of the degree of vitality in the test site was obtained by dividing the ratio value into six ranks as follows;

Value of ratio	—	2.5	—	5	—	8	—	12	—	16	—
Rank of vitality	1		2		3		4		6		6
	very low (dead)		low		warning		allowable		high		very high

Fig. 14 shows the results of the mapping of the degree of vitality in 1977 and 1980. As both images have been geometrically corrected, it is possible to overlay the forest type map of this site directly onto the evaluation map. As a result of this overlay, the following results have been obtained;

a) In most of the area of red pine, which is dominant in this site and the same tree species as the tree samples used for the experiment of section 4, the rank of vitality is 4 (allowable) both in 1977 and 1980.

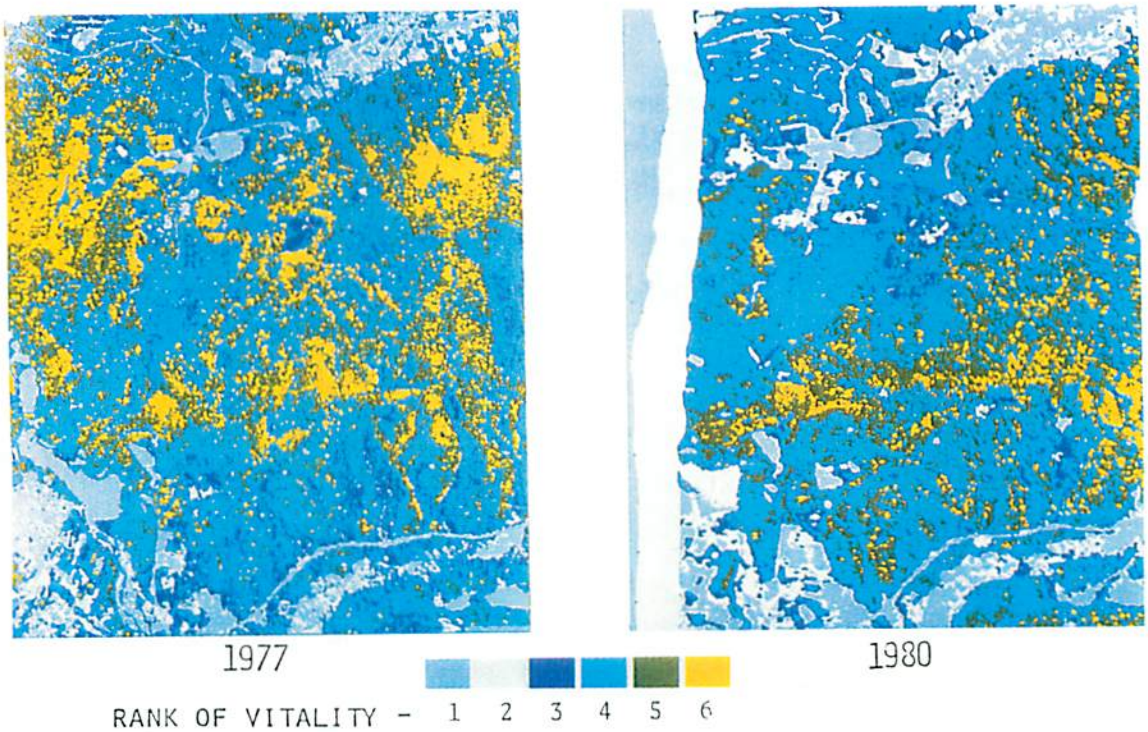

Fig. 14 Tree vitality degree maps in 1977 and 1980. The left side of the image in 1980 shows the lack of data due to course deviation.

b) Ranks below 3 can be seen only in the cut area, in very young age areas with very young trees, and in non-forested areas.

c) Ranks 5 and 6 (high and very high) correspond to the area of larch or broadleaf trees, both of which are deciduous.

d) The decrease of vitality rank from 1977 to 1980 occurs only in some areas of deciduous trees, while the rank of red pine remains constant.

The vitality change of deciduous trees is less important than that of evergreen trees because seasonal variation is considered to be the main reason for the change. In that sense, the continuous vitality of red pine is considered to suggest that there is no essential yearly change of the tree vitality condition in this test area.

7. Discussion

There exists a certain limitation concerning evaluation with a MSS in htis test area because MSS data have been acquired only once a year until now. The essential difficulty is to discriminate between seasonal variations and yearly variations. This problem might be resolved partly if the correspondence between the results of MSS data analysis and the actual forest types of the test area was studied in detail. Although more precise mapping techniques of MSS data onto a topographical map is necessary for the completion of the above study, the pre-processing techniques develoed in this study seem to offer a satisfactory data set for a semi-manual interpretative study of the relationship between tree vitality and the various forest types in the test area.

Another esential problem is verification for the evaluation of tree vitality itself. Most of the changes detected with the MSS are artificial changes which result from the management of forests, for example, the cutting of grass under trees and the cutting of some branches. Any abnormal (non-artificial) decrease of tree vitality has not been established in this area by either field survey or remote sensing. Thus, there is only the verification of a "no false-alarm" situation concerning natural tree vitality decrease at the present. In order to obtain real verification of the approach described in this paper, it is necessary to extend the test site to other sites where actual tree vitality decrease has been in progress, for example, where red pine has been damaged by pine bark beetles.

8. Conclusion

A technical approach using airborne MSS data for the evaluation of the condition of forest tree vitality has been studied for the purpose of environmental monitoring of a forested area under long tunnel construction. This study has been continued during the past four years and it will go on for a few more years. So far as this test area is concerned, there is the possibility of not detecting any actual tree vitality decrease as described in the previous section, which may be a reasonable result at the conclusion of monitoring of this test area. However, this is only a pilot study on the application of MSS data to the environmental monitoring of forested or other vegetation areas. Since the basic framework of the MSS data analysis system has been established by this study, the analytic tools developed in this study are expected to be utilized effectively in various environmental monitoring projects with the MSS data in the near future.

Acknowledgement

The authors wish to thank Prof. Emori of Chiba University, Dr. Tsuchiya of the Environmental Agency of Japan and Mr. Watanabe of the Japan Forest Technical Association for their advice and cooperation in this study.